

### Contents lists available at SciVerse ScienceDirect

# Physica B

journal homepage: www.elsevier.com/locate/physb



# Ion implantation induced defects in ZnO

L. Vines a,\*, J. Wong-Leung b, C. Jagadish b, E.V. Monakhov a, B.G. Svensson a

- a University of Oslo, Department of Physics/Centre for Materials Science and Nanotechnology, P.O. Box 1048 Blindern, N-0316 Oslo, Norway
- b Department of Electronic Materials Engineering, Research School of Physics and Engineering, The Australian National University, Canberra, ACT 0200, Australia

#### ARTICLE INFO

Available online 24 September 2011

Keywords:
Deep energy levels
Ion radiation effects
III-VI semiconductors
Point defects and defect clusters

#### ABSTRACT

N-type ZnO single crystals have been implanted with 500 keV  $\rm O^+$  and 1.2 MeV  $\rm Zn^+$  ions using doses between  $\rm 1 \times 10^{11}$  and  $\rm 2 \times 10^{12}$  cm $^{-2}$ , and the generation of deep-level defects in the upper part of the band gap has been studied by capacitance-voltage (CV) and deep level transient spectroscopy (DLTS) performed up to sample temperatures of 500 K. At least three implantation-related deep defects are observed by DLTS, with activation energies of 0.57, 0.97 and 1.2 eV below the conduction band edge. The generation of the two latter levels is pronounced in the reported samples, while the former has lower generation rate for O and Zn implantations compared to electrons and light ion irradiation. Moreover, a dramatic change in the depth distribution of charge carriers is observed, indicating acceptor generation or donor migration at or below 400 K.

© 2011 Elsevier B.V. All rights reserved.

# 1. Introduction

Zinc oxide (ZnO) is a wide band gap semiconductor ( $E_g \sim 3.4 \text{ eV}$ ) that has received considerable attention the last few years due to its potential applications in light emitting devices and photovoltaics. However, the technological advances of ZnO have been hindered by the difficulty in controlling and understanding the electrical behavior of intrinsic and impurity related defects. In particular, controlling charge carrier profiles by ion implantation has proven to be more difficult compared to e.g. Si technology, and remains a major challenge for the commercial production of ZnO based devices. This includes both dopant activation in the desired atomic configuration and defect control of ion induced damage, where deep-level defects acting as recombination or trapping centers may arise and considerably degrade the performance of the device. In this respect, intrinsic defects are of particular importance in ZnO, since many of the primary intrinsic defects are expected to be electrically active and a main contributing factor to the "native" n-type conduction. Oxygen vacancies  $(V_0)$ ,  $V_0$  complexes, Zn interstitial-related complexes, and residual impurities such as hydrogen and aluminium are all believed to be donors in ZnO, while oxygen interstitials  $(O_i)$ , Zn vacancies  $(V_{Zn})$  and their complexes are considered as acceptors [1,2]. However, experimental identification of the primary defects is still under debate.

Junction spectroscopic techniques are a crucial vehicle for probing the electrical properties of semiconductor materials and deep level transient spectroscopy (DLTS) is known to be one of the most sensitive characterization tools. However, only a rather

limited number of studies using these techniques partially due to the difficulty in producing high quality Schottky barriers. In an early study, Simpson and Cordaro reported a dominant defect level in hydrothermally grown ZnO at  $\sim E_C - 0.30$  eV ( $E_C$  denotes the conduction band edge), and this defect was later characterized and labelled E3 by Auret et al. [3,4]. E3 is found in all ZnO samples irrespective of the growth method and processing conditions, but shows only a minor response to electron and light ion irradiation. The most prominent deep level affected by H+ and He $^+$  irradiations, on the other hand, are found  $\sim 0.55$  eV below  $E_{\rm c}$  and its concentration hinges linearly on the ion dose [5–7]. For ion implantation studies of heavier ions, Schmidt et al. [8] found that a level at  $E_c$  – 0.19 eV increased after Zn implantation and subsequent annealing at 700  $^{\circ}\text{C.}$  Gu et al. [9] observed a level at  $E_c$  – 0.95 eV after N<sup>+</sup> implantation and annealing from 650 °C to 750 °C, and the appearance of a level at  $E_C$  –0.17 eV after anneals above 750 °C. However, identification and a thorough understanding of the defect behavior in ZnO is still lacking. For instance, the levels 0.30, 0.55, and 0.89 eV below  $E_c$  have all been tentatively assigned to  $V_0$ , and there is still no consensus in the literature.

Here we report on a DLTS study of defect generation after implanting oxygen and zinc in ZnO, with a particular emphasis on deep-level defects in the upper part of the band gap. By using matrix elements (self-ions) for implantation, we expect only generation of intrinsic defects. Both  $\rm O^+$  and  $\rm Zn^+$  implantations show similar defect generation. In particular, the generation of deep defects in the range 0.97–1.2 eV below  $E_c$  is pronounced. Moreover, the ion induced damaged region shows a restructuring at low temperatures, below 400 K, where a freeze out of charge carriers is observed.

<sup>\*</sup> Corresponding author.

E-mail address: Lasse.Vines@fys.uio.no (L. Vines).

## 2. Experimental

Wafers of hydrothermal and melt-grown ZnO from SPC Goodwill and Cermet, respectively, were cut in four  $5 \times 5$  mm samples. The samples were cleaned in aceton and ethanol, and treated for 1 min in boiling H<sub>2</sub>O<sub>2</sub>, before 100 nm Pd Schottky contacts were deposited using e-beam evaporation. The samples were implanted at room temperature using either 500 keV O<sup>+</sup> or 1.2 MeV Zn<sup>+</sup> ions with doses ranging from  $1 \times 10^{11}$  to  $2 \times 10^{12}$  cm<sup>-2</sup>. The projected range  $(R_p)$  of the oxygen and zinc ions in ZnO were 460 and 320 nm, respectively. DLTS measurements were carried out using a refined version of a setup described in detail elsewhere [10]. In short, the sample temperature was scanned from 77 to 450 K, where the capacitance transients were averaged within an interval of 1 K. The DLTS signal was extracted using a lock-in type of weighting function with six relatively long rate windows from  $(100 \text{ ms})^{-1}$  to  $(3.2 \text{ s})^{-1}$ , applying a reverse bias of typically -3 V and a filling pulse of +3 Vwith 50 ms duration.

## 3. Results and discussion

Fig. 1 shows the capacitance versus temperature for a typical sample before irradiation, measured using a reverse bias of -3 Vand probing frequencies between 60 kHz and 1 MHz, while the insets show the  $1/C^2$  (a) and current (b) versus voltage characteristics at room temperature. The average free carrier concentration was about  $5\times 10^{17}\,\text{cm}^{-3}$  in the sample shown, but varied from 2 to  $5\times$  $10^{17} \, \text{cm}^{-3}$  (before implantation). From inset (a) (Fig. 1) one can also observe that the  $1/C^2$ -curve is nonlinear indicating that the net carrier concentration is nonuniform in the near surface region with a reduction close to the metal interface. The capacitance is varying from 63 pF at 100 K to about 100 pF at 400 K using a reverse bias of -3 V, for a contact with diameter of 480  $\mu$ m, and the increase around 300 K can partially be explained by a release of carriers from a level around 0.3 eV below  $E_c$ . The current voltage measurements show a rectification of more than three orders of magnitude between -1 V and +1 V in applied bias voltage. Although the irradiation reduced the rectification in some of the samples, the rectification was

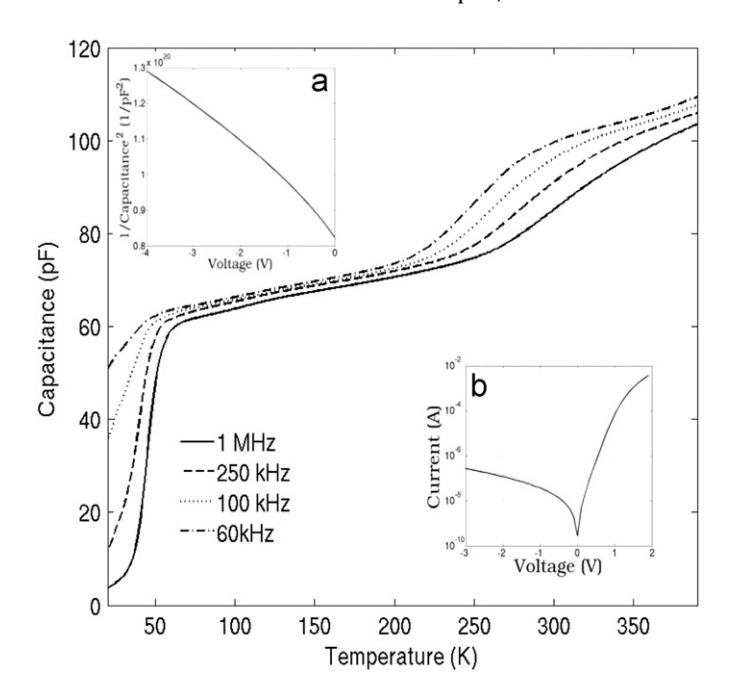


**Fig. 1.** Capacitance versus temperature for a typical sample before irradiation measured using a contact with a diameter of 480  $\mu$ m. Inset (a) shows  $1/C^2$  versus voltage, while inset (b) shows the current voltage characteristics.

still above two orders of magnitude for all samples, and sufficient for DLTS measurements at elevated temperatures.

The relatively high carrier concentration in the samples resulted in a narrow probing region for the applied bias voltage suitable for DLTS measurements (-3 V). With a projected range for both 500 keV and 1.2 MeV Zn ions in the  $\sim 400$  nm range, as obtained from SRIM simulations [11], only a part of the ion induced defect profiles were probed.

Fig. 2 shows DLTS spectra of the samples implanted with 500 keV  $O^+$  ions with doses of  $6 \times 10^{11}$  (low dose) and  $2 \times 10^{12}$  cm<sup>-2</sup> (high dose), and the measurements are carried out immediately after implantation. The signature of at least four defect levels is present in Fig. 2. labeled E2–E5, and with corresponding energy level positions of 0.15, 0.3, 0.55 and 0.97 eV below  $E_c$ . The apparent capture crosssections for E2, E3 and E4 were found to be  $8 \times 10^{-16}$ ,  $2 \times 10^{-15}$  and  $5 \times 10^{-13} \, \text{cm}^2$ , respectively. However, several of the defects are observed in unirradiated samples, i.e. E2, E3 and E5. The defect level E2 ( $E_c$  – 0.15 eV) has previously been observed in similar samples where the magnitude varies from wafer to wafer, and tentatively assigned to an impurity related complex [12]. The well-known level around  $E_c$  – 0.3 eV, normally labeled E3 [4], is found in a significant amount in the unimplanted samples. The DLTS amplitude of both E2 and E3 increase for the low dose compared to the unimplanted sample, while for the high dose a decrease of both E2 and E3 is observed. The level labeled E4, with an activation energy of  $E_c$  – 0.57 eV, has also previously been reported [4], and tentatively assigned to the oxygen vacancy  $(V_0)$  [13], with a strong dependence on H<sup>+</sup> and He<sup>+</sup> irradiation doses. However, Figs. 2 and 3 reveal a low generation rate of E4, in accordance with reported data on Zn implanted and annealed samples [8]. Less is known about the defect level labelled E5; the position is 0.97 eV, with an apparent capture cross-section of  $2 \times 10^{-14}$  cm<sup>2</sup>. The level has previously not been observed in the hydrothermally grown samples, but may be of the same origin as a level reported by Gu et al. [9] in a nitrogen implanted and annealed (650 °C) pn junction structure. E5 is present in unirradiated samples, but shows a strong dependence of the implantation dose, where both the medium and high doses exceed the quantitative limits of the DLTS technique. Thus, only qualitative features are discussed

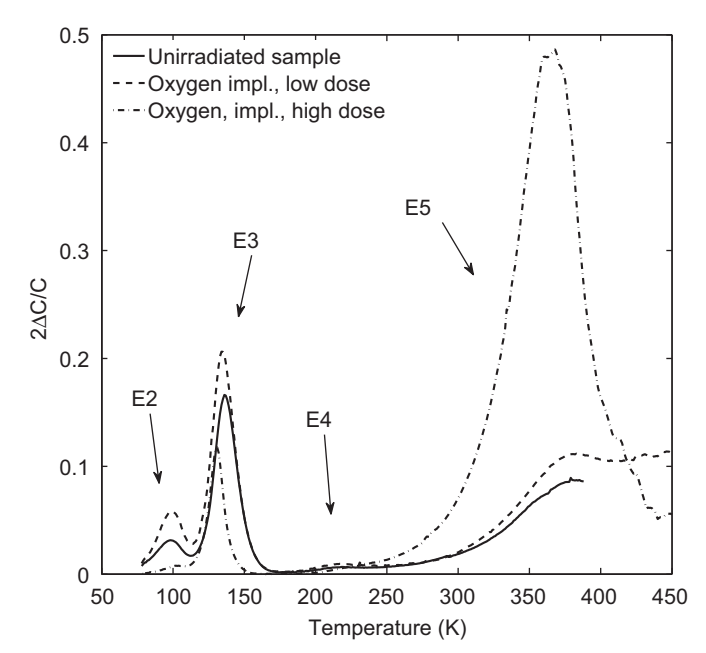


**Fig. 2.** DLTS signal  $(\Delta C/C)$  of hydrothermally grown samples implanted by 500 keV  $0^+$  ions with doses  $6\times 10^{11}$  and  $2\times 10^{12}$  cm $^{-2}$ , using a rate window of  $(3.2\text{ s})^{-1}$ .

# Download English Version:

# https://daneshyari.com/en/article/1810721

Download Persian Version:

https://daneshyari.com/article/1810721

<u>Daneshyari.com</u>